

**Electronic supplementary information**

**GSH-triggered size increase of porphyrin-containing nanosystems for  
enhanced retention and photodynamic activity**

Jianxu Zhang,<sup>a,b</sup> Xiaohua Zheng<sup>a,b</sup> Xiuli Hu<sup>a</sup> and Zhigang Xie<sup>a,\*</sup>

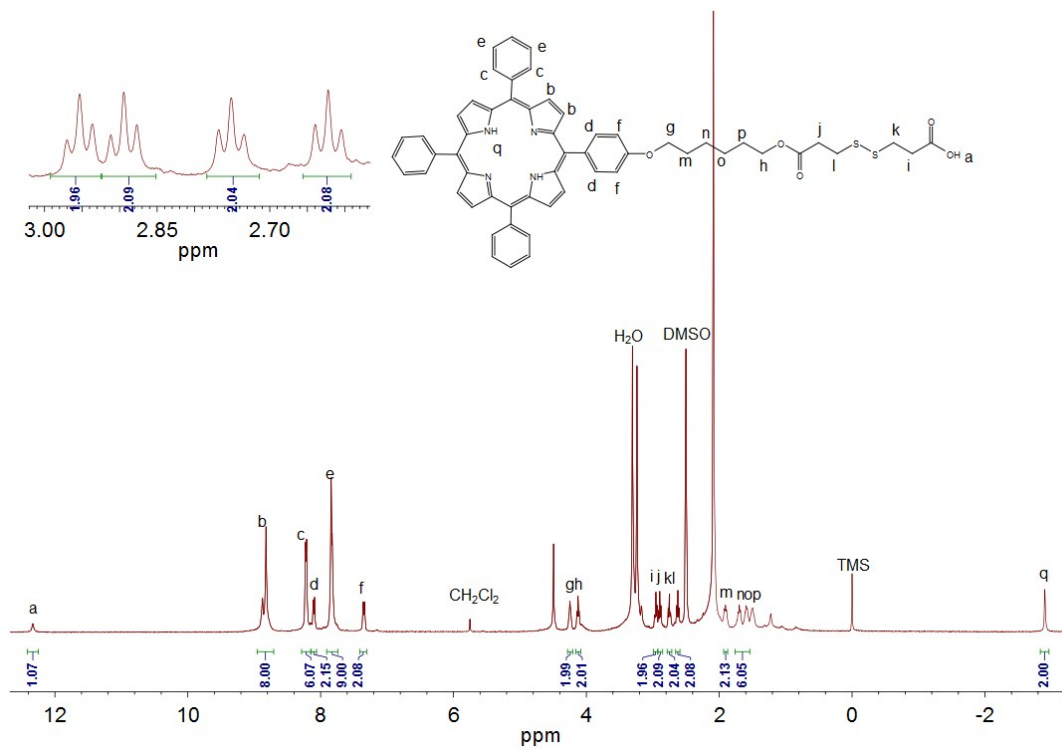


Figure S1.  $^1\text{H}$  NMR spectrum of TPP 1 in DMSO.

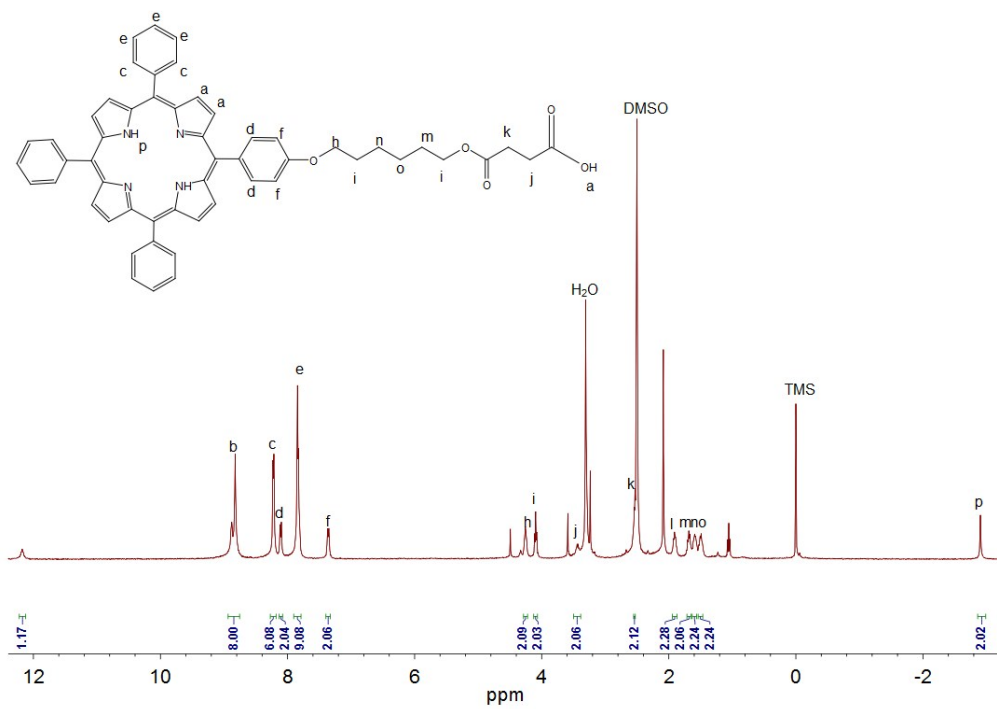
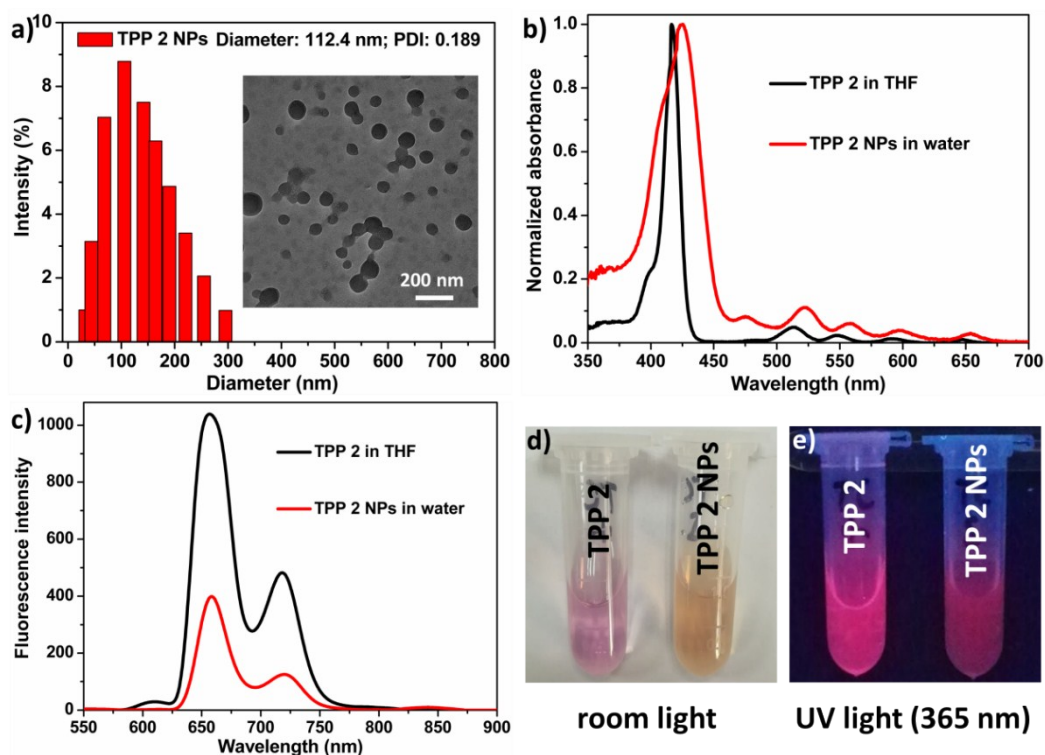
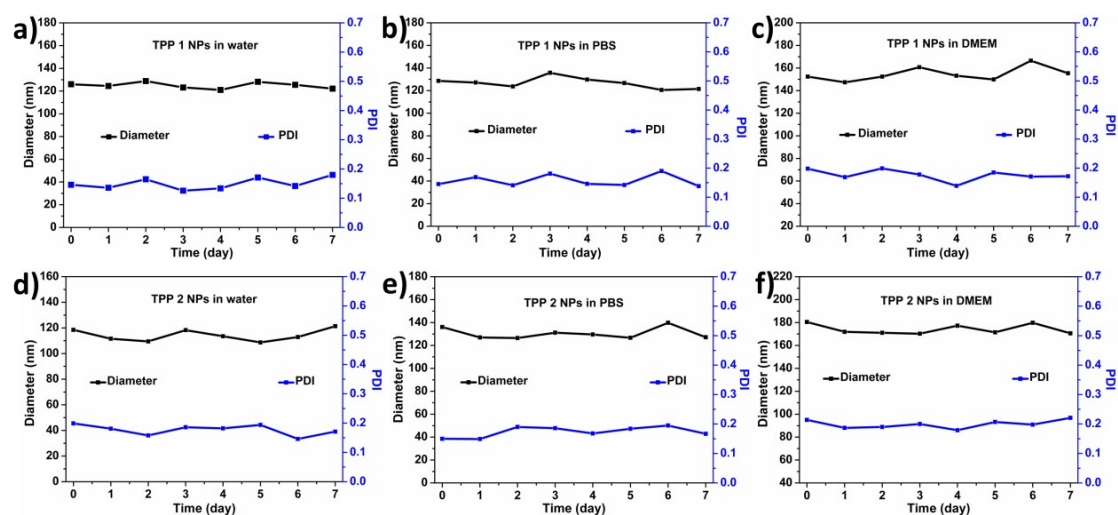


Figure S2.  $^1\text{H}$  NMR spectrum of TPP 2 in DMSO.



**Figure S3.** a) DLS intensity-weighted diameter of TPP 2 NPs. Insets: TEM image of TPP 2 NPs. Scale bar in TEM image: 200 nm. b) Absorbance spectra and c) PL (excited at 420 nm) spectra of TPP 2, and TPP 2 NPs, respectively. d) and e) Photographs of TPP 2 in THF and TPP 2 NPs in water under room light (left picture) and UV light (right picture), respectively.



**Figure S4.** The stability of size distribution of TPP 1 NPs and TPP 2 NPs in different conditions during seven days. a) TPP 1 NPs in water; b) TPP 1 NPs in PBS; c) TPP 1 NPs in DMEM; d) TPP 2 NPs in water; e) TPP 2 NPs in PBS and f) TPP 2 NPs in DMEM, respectively.

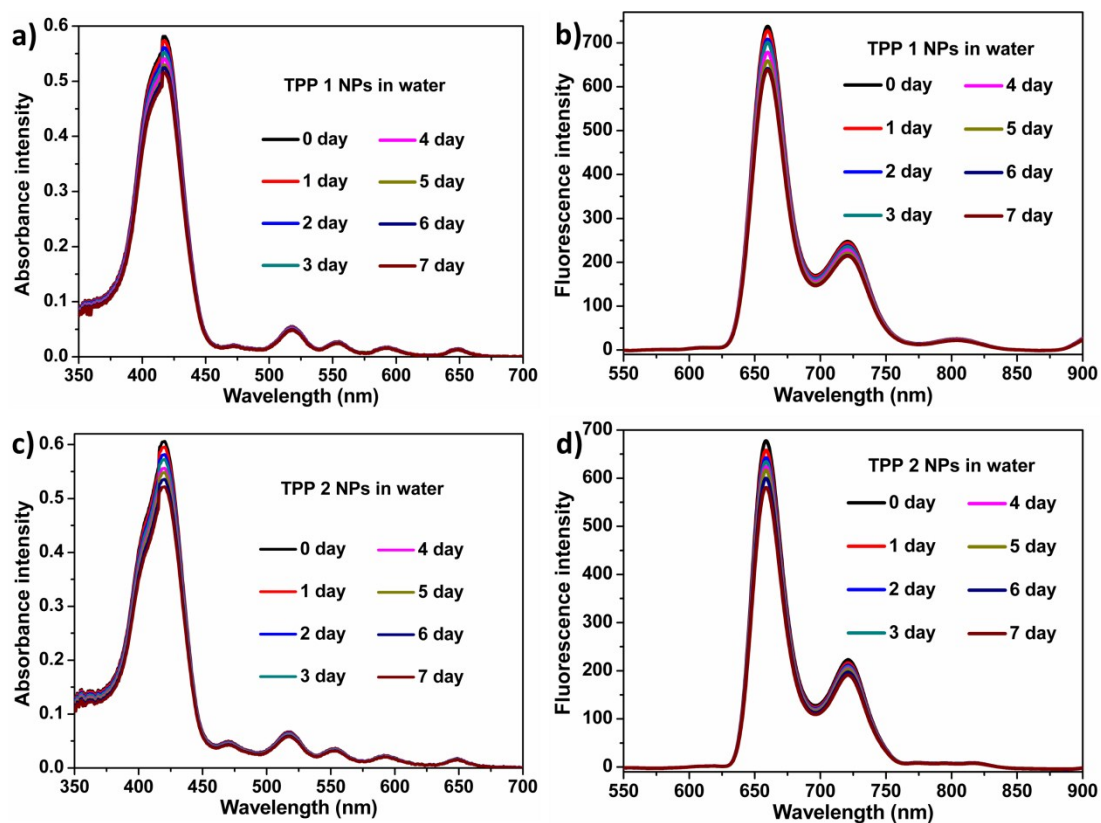


**Figure S5.** a) The stability of absorbance intensity and b) fluorescence intensity of TPP 1 NPs during seven days, respectively. c) The stability of absorbance intensity and d) fluorescence intensity of TPP 2 NPs during seven days, respectively.

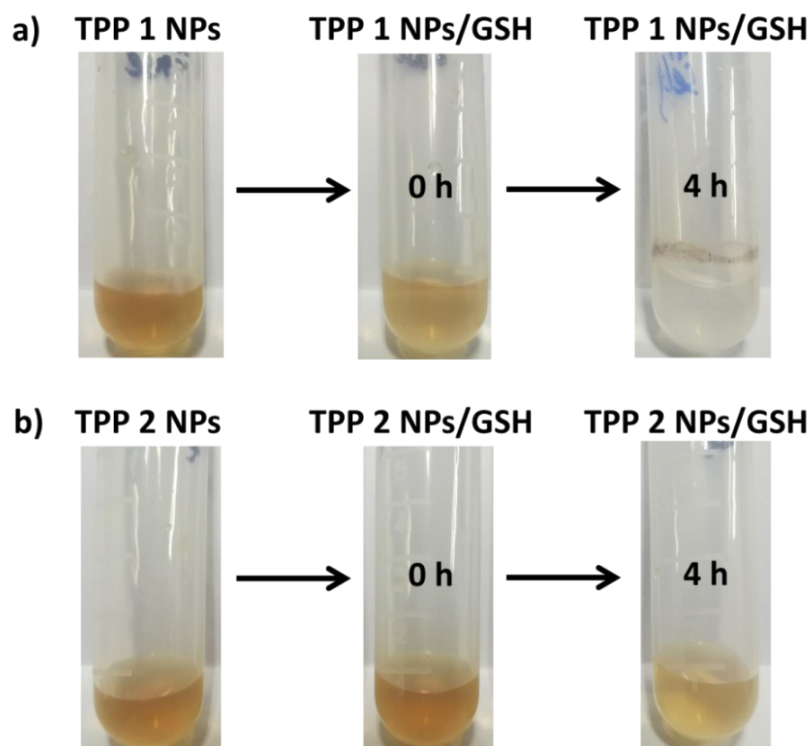


**Figure S6.** The picture of a) TPP 1 NPs and b) TPP 2 NPs treated with 10mM GSH for 0 h and 4 h, respectively.

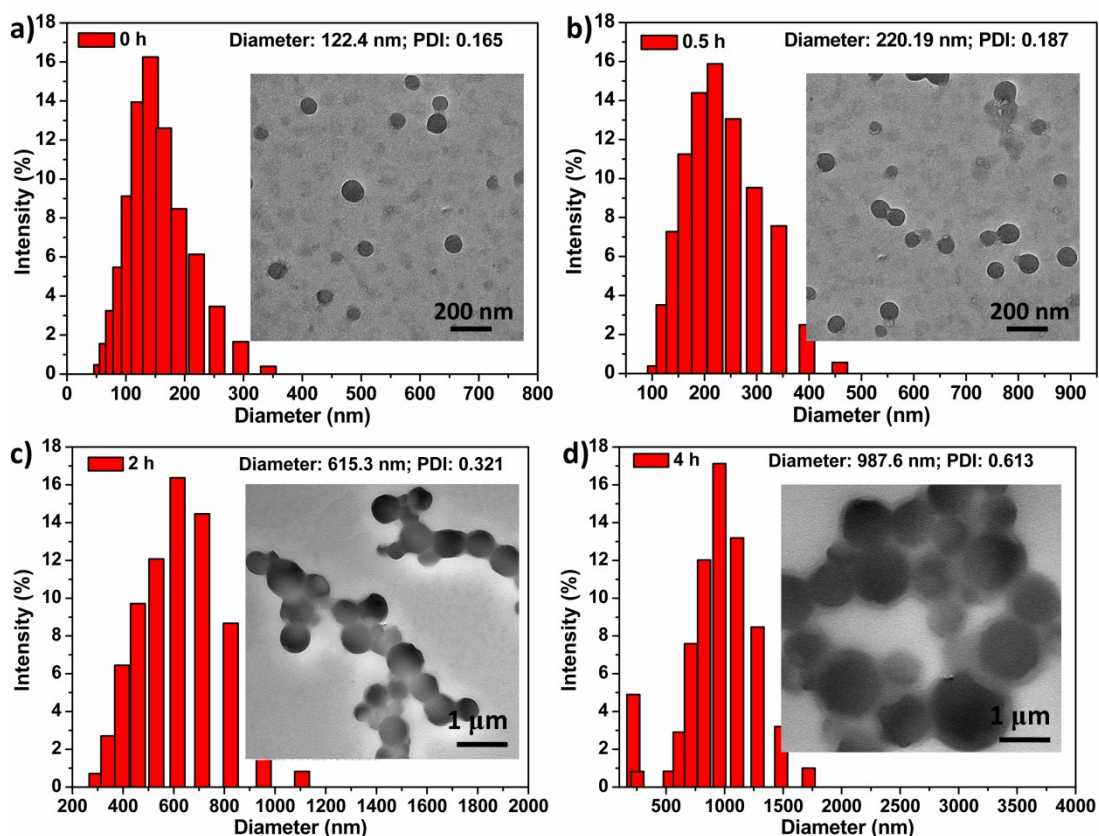


**Figure S7.** DLS intensity-weighted diameter of TPP 1 NPs after treated with GSH at varied time periods. Insets: TEM image of TPP 1 NPs after treated with GSH at varied time periods. Scale bars in a) and b) are 200 nm, and that of c) and d) are 1  $\mu$ m. a) TPP 1 NPs after treated with GSH at 0 h. b) TPP 1 NPs after treated with GSH at 0.5 h. c) TPP 1 NPs after treated with GSH at 2 h. d) TPP 1 NPs after treated with GSH at 4 h.

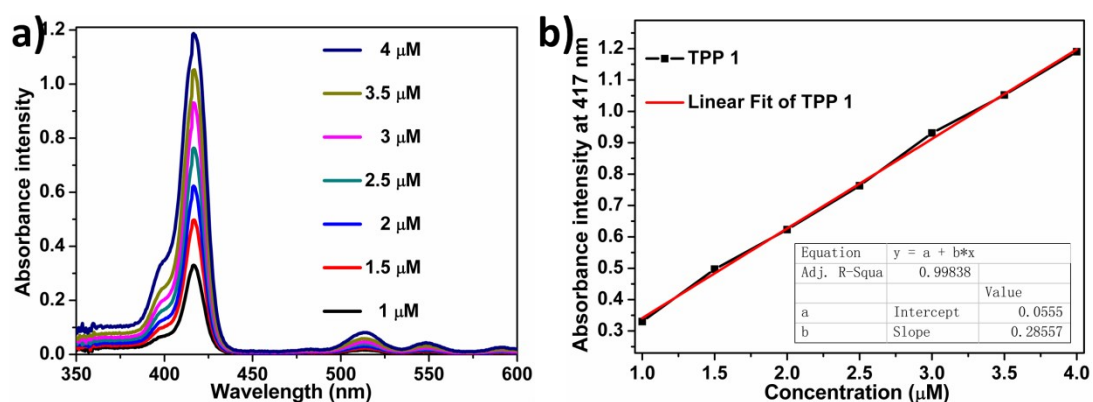


**Figure S8.** a) and b) Standard absorbance curve of TPP 1. (The absorbance of TPP 1 molecules at 417 nm (from a mixture of THF and water (v/v = 4:1)) as a function of TPP 1 concentration.)

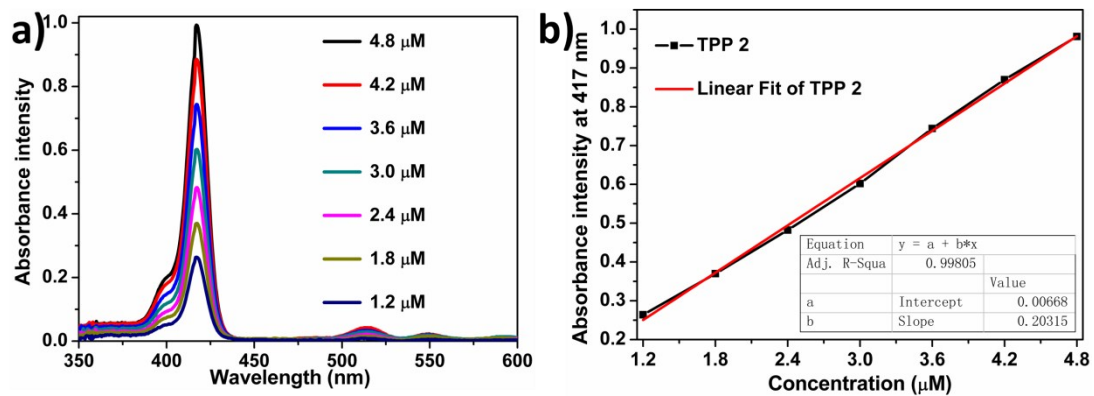


**Figure S9.** a) and b) Standard absorbance curve of TPP 2. (The absorbance of TPP 2 molecules at 417 nm (from a mixture of THF and water (v/v = 4:1)) as a function of TPP 2 concentration.)

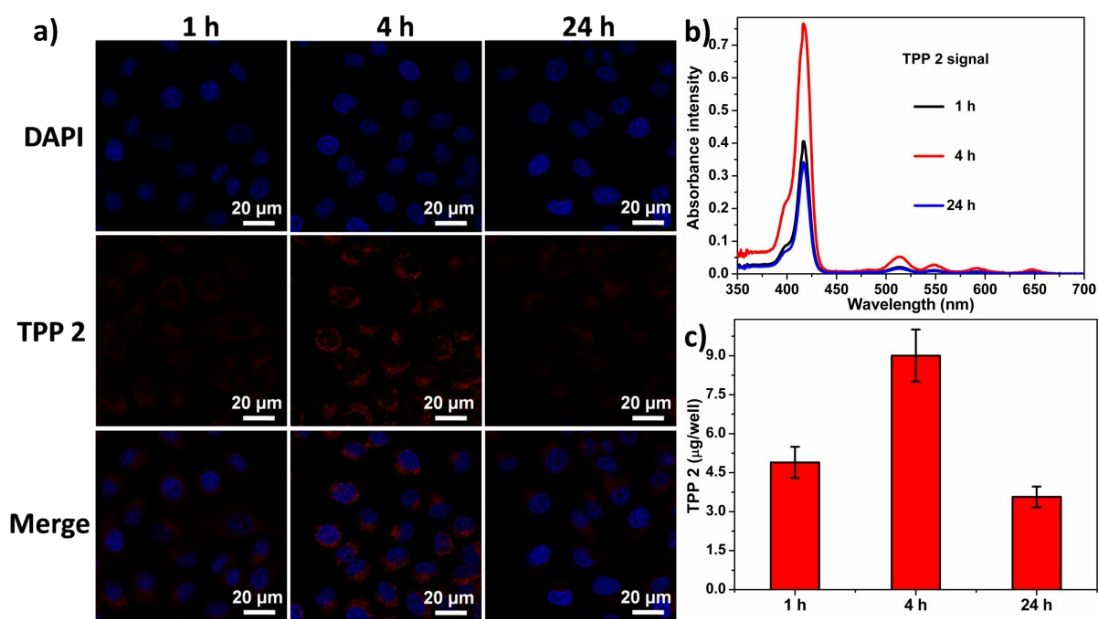


**Figure S10.** a) CLSM images showing changes in the signal of TPP 2 in HeLa cells treated with TPP 2 NPs with the same TPP 2 concentration of 20 μM for 1 h (left), 4 h (middle) at 37 °C, and the right picture was HeLa cells treated with TPP 2 NPs for 4 h and replaced by fresh DMEM for another 24 h incubation. Scale bars: 20 μm. Absorbance of b) TPP 2 of the TPP 2 NPs internalized by HeLa cells after 1, 4, and 24 h incubation. c) Quantitative analysis of b) by standard absorbance curve of TPP 2.

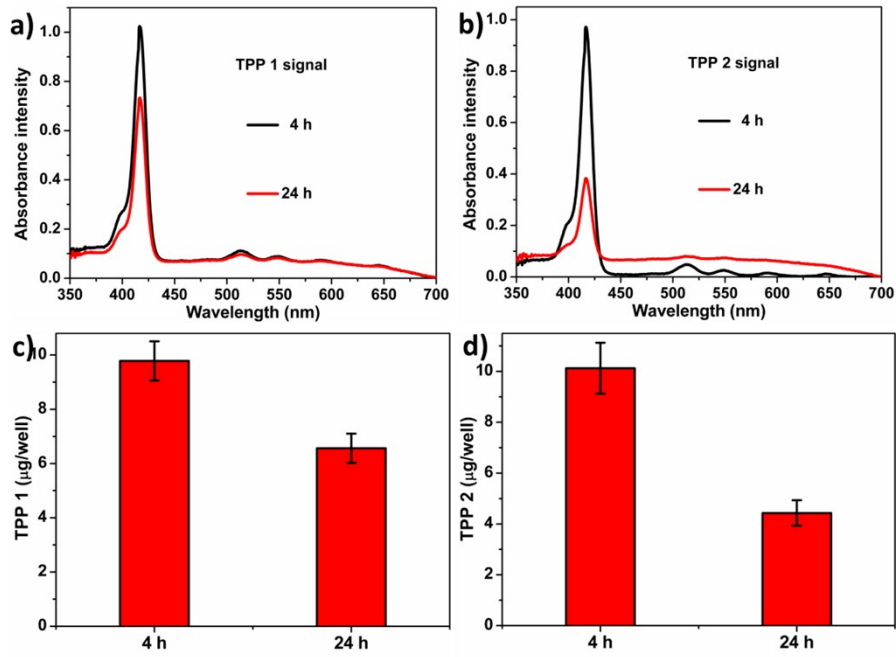


**Figure S11.** Absorbance of a) TPP 1 and b) TPP 2 internalized by HeLa cells pretreated with 10 mM GSH after 4 and 24 h incubation, respectively. c) and d) Quantitative analysis of a) and b) by standard absorbance curve of TPP 1 and TPP 2, respectively.

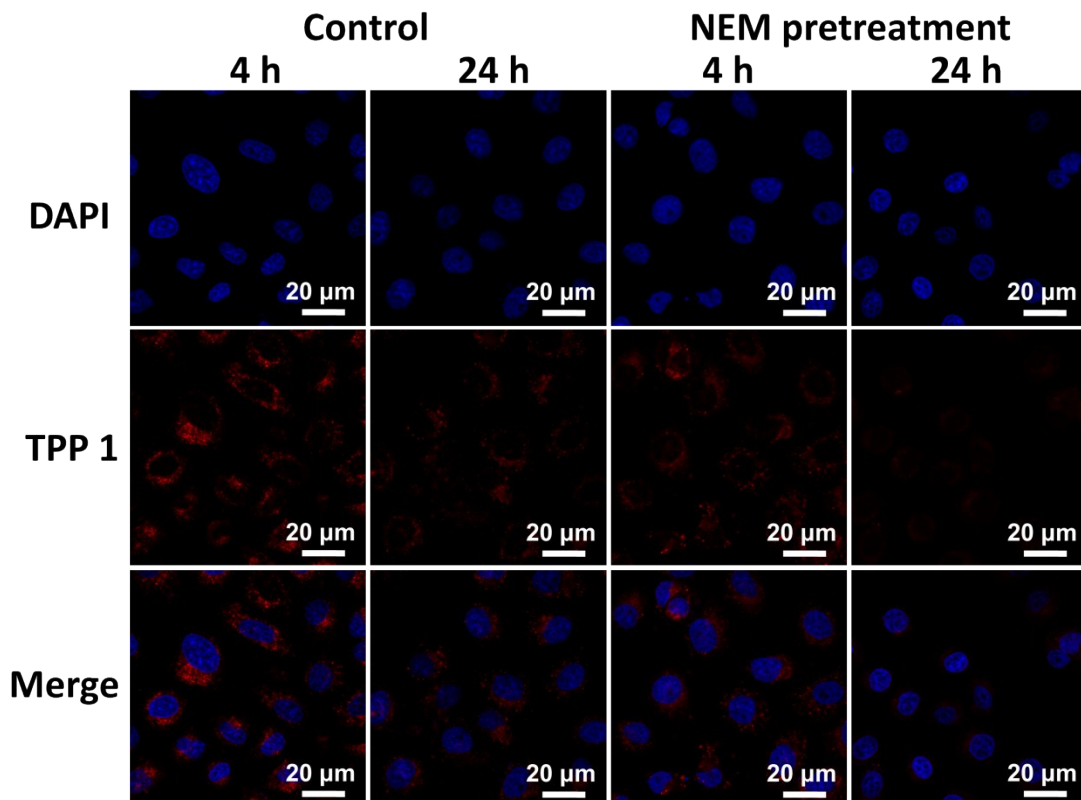


**Figure S12.** CLSM images showing changes in the signal of TPP 1 in HeLa cells pretreated with 1 mM NEM after treated with TPP 1 NPs with the same TPP concentration of 20 µM for 4 h and replaced the medium by fresh DMEM for another 24 h incubation. Scale bars: 20 µm.

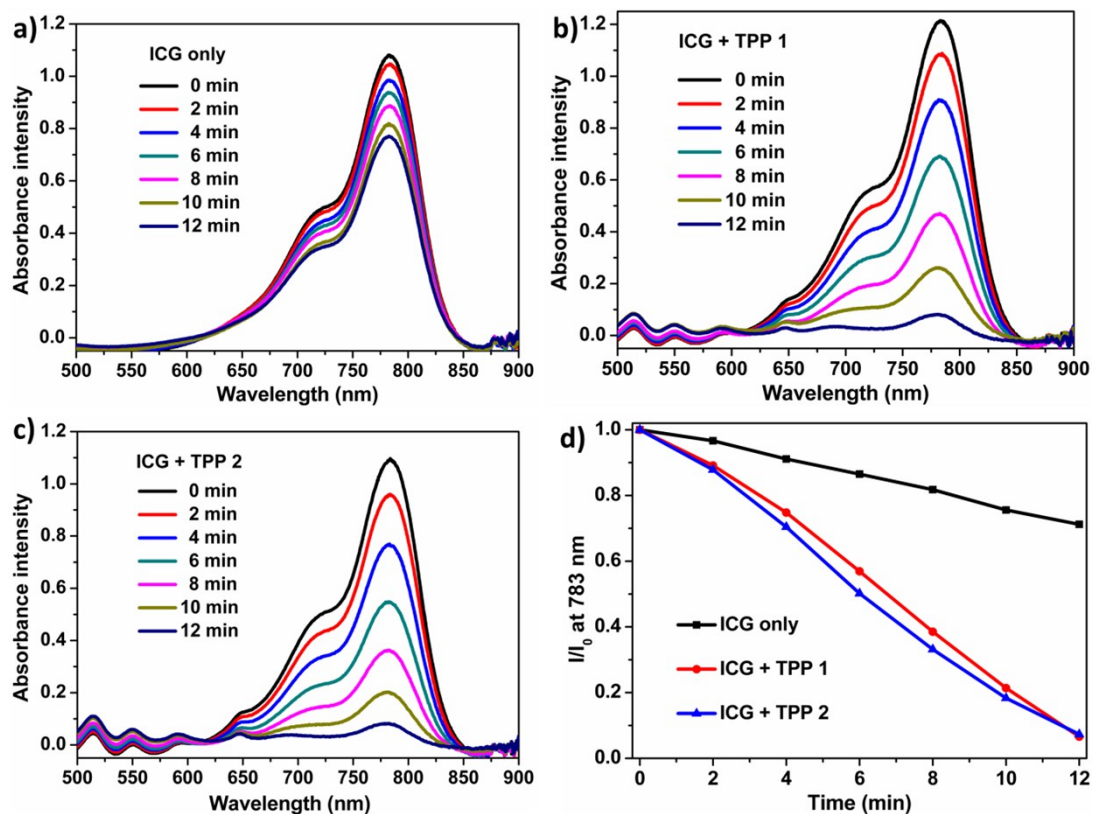


**Figure S13.** a) Time-dependent absorption spectra of ICG alone upon irradiation in DMF. Time-dependent absorption spectra of ICG upon irradiation in the presence of b) TPP 1 and c) TPP 2 in DMF, respectively. d) Comparison of the decay rate of ICG alone (black line) and of ICG in the presence of TPP 1 (red line) and TPP 2 (blue line), respectively.

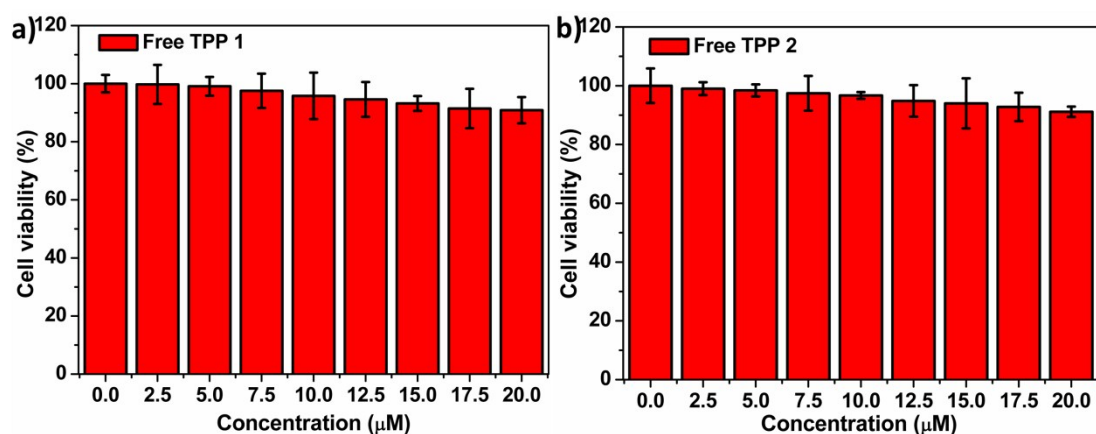


**Figure S14.** Relative cell viabilities of HeLa cells incubated with different concentrations of a) TPP 1 and b) TPP 2, respectively.

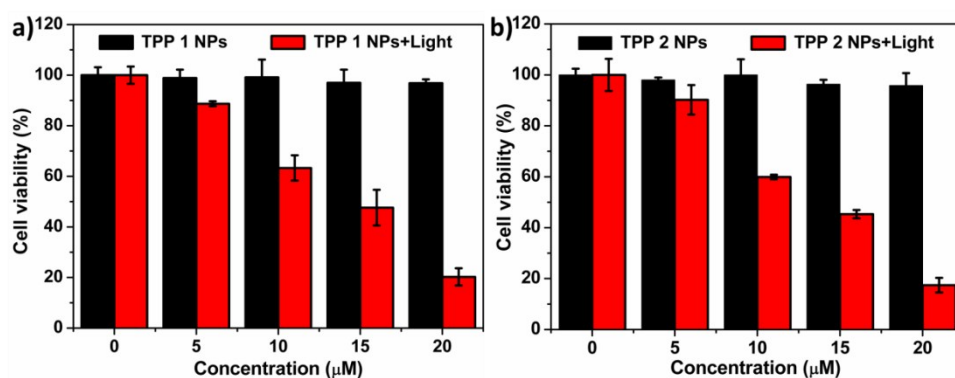


**Figure S15.** Relative cell viabilities of HeLa cells incubated with different concentrations of a) TPP 1 NPs and d) TPP 2 NPs for 4 h with or without laser irradiation, respectively.

To visually demonstrate the efficiency of GSH-triggered enhanced retention of TPP 1 NPs in photodynamic therapy, we studied the morphology changes of HeLa cells after different treatments, respectively. As shown in **Figure S15** and **Figure S16**, compared to the control group, TPP NPs alone or only light irradiation did not affect cell morphology, which agreed well with the MTT experiments (shown in Figure S14). After incubating with TPP 1 NPs or TPP 2 NPs for 4 h, the cells under irradiation showed significantly morphology changes (Figure S15). These results suggested TPP NPs had great promise as a nanosystem for photodynamic therapy. Within GSH pretreatment, after incubated with TPP 1 NPs for 4 h and replaced the medium by fresh DMEM for another 24 h incubation, light irradiation was still able to cause the obvious morphology changes (Figure S16a), indicating there were enough TPP 1 in cells to generate  $^1\text{O}_2$  under irradiation. In contrast, the cells treated with TPP 2 NPs displayed unobvious morphology changes with light irradiation, illustrating the insufficient retention of TPP 2 in cells (Figure S16b). These results suggested that TPP 1 NPs could effectively kill the cancer cells under irradiation through GSH triggered enhanced cellular retention.

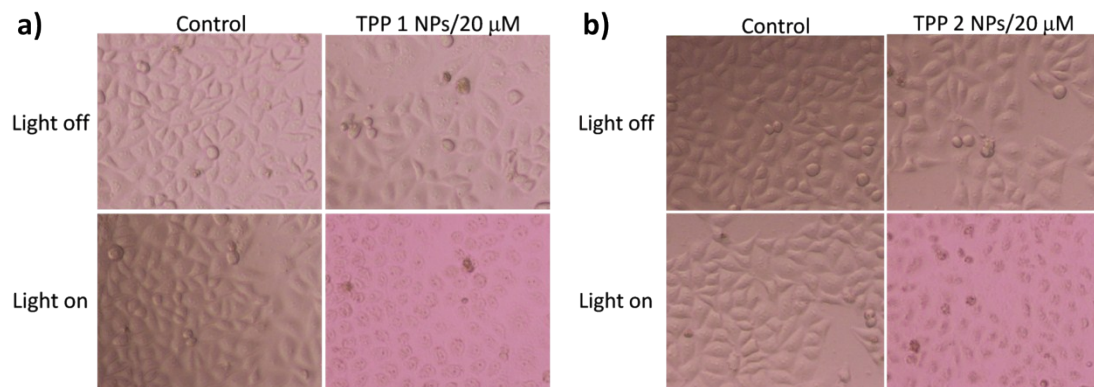


**Figure S16.** The morphology change of HeLa cells incubated with 20  $\mu\text{M}$  a) TPP 1 NPs or b) TPP 2 NPs for 4 h with and without laser irradiation.

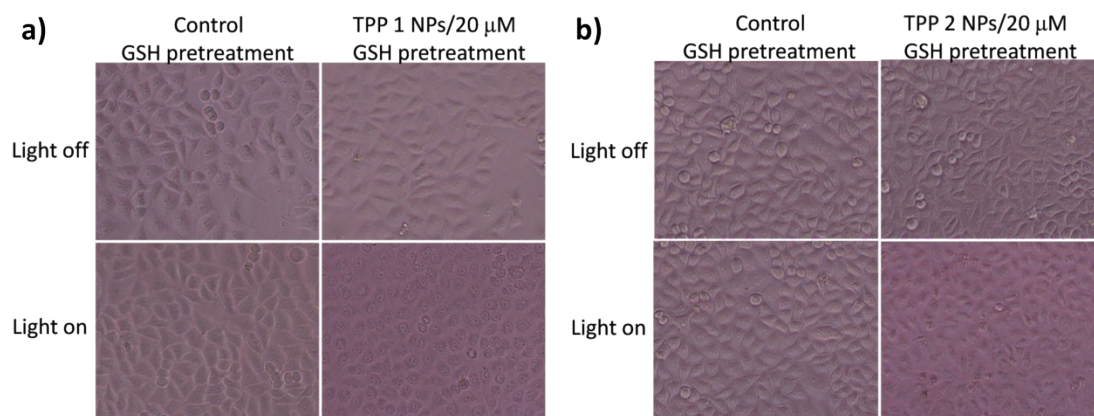


**Figure S17.** The morphology change of HeLa cells incubated with 20  $\mu\text{M}$  a) TPP 1 NPs or b) TPP 2 NPs for 4 h and replaced the medium by fresh DMEM for another 24 h incubation, with and without laser irradiation.